Acta Ophthalmologica

Correlation of the KISA% index and Scheimpflug tomography in 'normal', 'subclinical', 'keratoconus-suspect' and 'clinically manifest' keratoconus eyes

Johannes Steinberg,[1,2] Silke Aubke-Schultz,[1] Andreas Frings,[1] Jan Hülle,[3] Vasyl Druchkiv,[1] Gisbert Richard,[1] Toam Katz[1,2] and Stephan J. Linke[1,2]

[1]Department of Ophthalmology, UKE - University Medical Center Hamburg-Eppendorf, Hamburg, Germany
[2]Care-Vision Germany, University Medical Center Hamburg-Eppendorf, Hamburg, Germany
[3]South West Peninsula Postgraduate Medical Education, School of Ophthalmology, Plymouth, UK

ABSTRACT.

Purpose: **To analyse tomographic changes in eyes classified as 'normal', 'keratoconus-suspect' and 'clinically manifest keratoconus' based on the established KISA% definition of Rabinowitz and Rasheed and to develop the category of 'subclinical keratoconus eyes' to expand the classification into a 'subtopographic' range.**

Methods: **Tomographic and topographic analyses of 670 eyes performed with a rotating Scheimpflug imaging system (Pentacam®, Oculus Inc., Wetzlar, Germany) were retrospectively analysed. Based on the KISA% keratoconus classification system, eyes were assigned to a 'normal', 'keratoconus-suspect' or 'manifest keratoconus' group. In addition, a new group of 'subclinical keratoconus eyes' was analysed, comprising unsuspicious fellow eyes of patients with keratoconus. T-tests, Wilcoxon rank-sum test, receiver operating characteristics (ROC) and robust regression analyses were performed to correlate tomographic parameters with the increasing KISA% index.**

Results: **KISA%-grouped keratoconus eyes showed robust tomographic changes. By adding the subclinical group, although the concurrent topography was unchanged, we were able to demonstrate statistically significant changes for almost all tomographic parameters (parameters with highest sensitivity/specificity: ART_max, [0.69/0.69], BAD_D [0.66/0.66]). The highest coefficient of determination (R^2) with the KISA% index was demonstrated for Ele_f_max ($R^2 = 0.70$), Ele_f_TP ($R^2 = 0.69$), Ele_b_TP ($R^2 = 0.69$) and BAD_D ($R^2 = 0.68$).**

Conclusion: **We recommend the use of the expanded KISA% index (eKISA% index) as the basis for the definition of keratoconus and normal groups in future keratoconus research projects.**

Key words: classification system – keratoconus – KISA% – subclinical keratoconus – tomography

Acta Ophthalmol. 2015: 93: e199–e207

© 2015 Acta Ophthalmologica Scandinavica Foundation. Published by John Wiley & Sons Ltd

doi: 10.1111/aos.12590

Introduction

'Keratoconus is a bilateral non-inflammatory corneal ectasia with an incidence of approximately 1 per 2000 in the general population. It has well-described clinical signs, but early forms of the disease may go undetected unless the anterior corneal topography is studied.' Referring to the web of science® (Thomson Reuters) these words, written by Rabinowitz in 1998, introduce the most cited publication in the field of keratoconus research (Rabinowitz 1998). Based on his assessment, Rabinowitz developed the topography-based KISA% index. This index describes the asymmetry of the corneal surface based on universal and easily calculable topographic parameters (Rabinowitz & Rasheed 1999).

Since then, new diagnostic techniques for the cornea (corneal tomography, wavefront and biomechanical analyses) have evolved with which keratoconus can be identified earlier than Rabinowitz would probably have imagined in 1998 (Pinero et al. 2012; Ali et al. 2014; Buhren et al. 2014). With these techniques keratoconus can now be identified on a subclinical level, that is before topographic changes (and, therefore, a reduction of the visual acuity) occur. To analyse changes on a subclinical level, it is essential to differentiate properly between 'normal' eyes and those with

Table 1. Analysed tomographic parameters.

Parameter	Unit	Definition/explanation
TPCT	μm	Corneal thickness at the thinnest point.
CCT	μm	Central corneal thickness (corneal thickness at the apex).
Ele_f_AP	μm	Front surface elevation at the corneal apex. *
Ele_f_TP	μm	Front surface elevation at the thinnest point. *
Ele_f_max	μm	Front surface elevation at the point with highest value within the 4-mm (diameter) zone centred at the apex. *
Ele_b_AP	μm	Back surface elevation at the corneal apex.†
Ele_b_TP	μm	Back surface elevation at the thinnest point.†
Ele_b_max	μm	Back surface elevation at the point with highest value within the 4-mm (diameter) zone centred at the apex.†
BAD_D		Belin-Ambrosio's BAD classification index combining elevation based and pachymetric corneal evaluation in one comprehensive display to give a global view of the tomographic structure of the cornea. Deviation of normality values were implemented for the front- and back-enhanced elevations, pachymetric distribution and vertical displacement of the thinnest in relation to the apex. The final BAD_D was developed to give lower than 5% of false positives and false negatives (Ambrosio 2010)
ART avg, ART max, ART min		Average/maximal/minimal 'Ambrósio Relational Thinnest' index. The 'ART' index displays the thinnest pachymetric value divided by the pachymetric progression, facilitating the identification of an abnormal cornea despite its thinnest value (Ambrosio 2010)
rpi_avg		Average pachymetric progression index. The rpi is calculated for every 1° meridian along the complete 360°, starting at the thinnest point. The RPI_avg displays the average of all meridians (Ambrosio 2010; Ambrosio et al. 2011). rpi will be higher if the cornea gets thicker in a more accentuated pattern from the thinnest point out to the periphery
rpi_max		Pachymetric progression index of the meridian with the strongest corneal thickness increase from the thinnest point to the periphery (Ambrosio 2010; Ambrosio et al. 2011)
rpi_min		Pachymetric progression index of the meridian with the minimal corneal thickness increase from the thinnest point to the periphery.
CV_3 mm, CV_5 mm, CV_7 mm, CV_10 mm	mm^3	Corneal volume calculated for a diameter of 3, 5, 7 or 10 mm centred at the corneal apex.

* Reference surface is the best-fit sphere of the central 8 mm (diameter) of the corneal front surface centred at the corneal apex.
† Reference surface is the best-fit sphere of the central 8 mm (diameter) of the corneal back surface centred at the corneal apex.

early keratoconus stages. A drawback of many recent studies addressing keratoconus is the difference in their inclusion and exclusion criteria for 'normal eyes' and 'subclinical' and 'clinically manifest' keratoconus.

This study analyses tomographic changes of 'normal', 'keratoconus-suspect' and 'clinically manifest' keratoconus eyes based on the definition of Rabinowitz and Rasheed (Rabinowitz & Rasheed 1999). In the light of the current diagnostic techniques, we decided to add the category 'subclinical keratoconus', thereby expanding the established KISA% classification to a 'subtopographic' level. A subclinical keratoconus eye was defined as an unsuspicious fellow eye (KISA% <60) of a patient with a manifest keratoconus on the other eye (KISA% >100). The aim of this study was to correlate KISA% with tomographic changes to provide data for an expanded KISA% (eKISA%) classification to supplement the established and easily calculable KISA% index, which can then be used as the basis for future research on the field of keratoconus.

Materials and Methods

This retrospective study was performed as part of a co-operation between the Care Vision Eye Clinics in Germany and Austria and the Department of Ophthalmology, University Medical Center Hamburg-Eppendorf. Tomographic and topographic analyses of patients with non-keratoconus ('normal') eyes and patients with keratoconus were retrospectively evaluated. The measurements were performed with a rotating Scheimpflug imaging system (Pentacam®, Oculus Inc.). The patients were instructed to keep both eyes open and fixate on the black target in the centre of the blue fixation beam. After attaining perfect alignment, the instrument automatically took a single scan comprising 25 Scheimpflug images within 2 second. The Pentacam® then reports the quality of the examination based on the size of the analysed area, the percentage of valid data, missing segments, deviation of the '3D model', deviation of the position of the cornea (x-, y- and z-axes) and eye movement. If the scan obtained an overall quality specification grade of 'OK' or '3D model', it was saved; if not, it was repeated. The quality grade '3D model' indicates a deviation of the anterior and posterior corneal surface from the physiological corneal shape. This typically occurs in eyes with advanced keratoconus. If a grade of '3D model' was reached, the analysis was evaluated further. The analysis was only included into statistical analysis if the result of the '3D model' quality was marked with a yellow display (red-marked analysis, suggesting a poor-quality analysis due to missing or miscalculated data, were excluded). Due to rigorous quality grading recruitment, 301 eyes had to be excluded.

As described by Rabinowitz, the KISA% index is a topography-based index to quantify the asymmetry of the corneal surface (Rabinowitz & Rasheed 1999). It is derived from the product of 4 indices: the K value, an expression of central corneal steepening; the I–S value, an expression of inferior–superior dioptric asymmetry; the AST index, which quantifies the degree of regular corneal astigmatism (Sim K1/Sim K2); and the skewed radial axis (SRAX) index, an expression of irregular astigmatism occurring in keratoconus (Rabinowitz 1995). The methods by which they are calculated and the calculation of the KISA% index itself were described in detail by Rabinowitz and Rasheed (Rabinowitz 1995; Rabinowitz & Rasheed 1999). The final index is calculated as:

$$\mathrm{KISA}\% = (\mathrm{K} \times \mathrm{I} - \mathrm{S} \times \mathrm{AST} \times \mathrm{SRAX} \times 100)/300$$

Based on the KISA% index, our groups were defined as follows: group

Table 2. Descriptives of the analysed parameters and their distribution within the normal and keratoconus groups.

	Normal eyes (n = 196) (group I)				Subclinical eyes (n = 146) (group II)				Keratoconus-suspect (n = 35) (group III)				Manifest keratoconus (n = 293) (group IV)			
Parameter (unit)	Mean	SD	Median	Q25/Q75	Mean	SD	Median	Q25/Q75	Mean	SD	Median	Q25/Q75	Mean	SD	Median	Q25/Q75
Age	33	11	32	25/41	34	11	32	26/43	35	13	35	26/44	34	12	32	25/43
K1 (D)	43.2	1.5	43.1	42.1/44.2	43.0	1.9	42.9	41.9/44.3	43.5	1.9	43.3	42.3/44.6	46.9	5.7	45.4	43.3/49.2
K2 (D)	44.6	1.8	44.6	43.4/45.7	44.4	2.3	44.1	43.0/45.8	46.1	2.7	45.4	44.3/48.5	50.6	6.4	49.2	46.4/52.9
Astig (D)	1.4	1.1	1.1	0.7/1.8	1.4	1.4	1.0	0.6/1.8	2.5	1.9	1.7	0.9/4.4	3.8	2.4	3.3	2.1/4.9
Kmax (D)	45.3	2.0	45.2	43.9/46.3	45.9	2.9	45.5	44.0/47.2	49.0	3.5	48.8	46.3/51.0	57.1	8.7	55.3	51.8/60.3
BAD_D	1.3	1.3	1.0	0.6/1.6	2.4	1.8	2.2	1.1/3.2	4.6	2.5	4.7	3.1/5.8	11.2	7.8	9.8	6.8/13.0
BFS front* (mm)	7.8	0.3	7.8	7.6/8.0	7.8	0.3	7.9	7.6/8.0	7.7	0.3	7.8	7.5/7.9	7.3	0.5	7.4	7.1/7.7
BFS back* (mm)	6.4	0.2	6.4	6.2/6.6	6.5	0.3	6.5	6.3/6.7	6.4	0.3	6.4	6.2/6.6	6.0	0.5	6.1	5.8/6.3
Ele_f_Apex*(μm)	2.4	2.1	2.0	1.0/3.0	2.6	2.6	2.0	1.0/4.0	4.7	5.1	3.0	1.0/9.0	12.1	13.1	10.0	3.0/16.0
Ele_f_TP*(μm)	2.8	3.2	2.0	1.0/4.0	5.0	4.5	4.0	2.0/7.0	9.3	7.3	10.0	6.0/14.0	28.6	21.9	26.0	18.0/38.0
Ele_f_max*(μm)	6.0	3.6	5.0	3.0/7.0	7.8	5.1	7.0	5.0/10.0	14.2	5.6	14.0	10.0/18.0	35.4	17.3	31.0	23.0/43.0
Ele_b_Apex*(μm)	3.2	4.8	2.0	1.0/4.0	4.6	7.2	3.0	0.0/7.0	12.5	13.7	10.0	0.0/25.0	28.5	28.6	22.0	10.0/41.0
Ele_b_TP*(μm)	7.0	8.0	5.0	3.0/9.0	13.9	12.5	11.0	5.0/22.0	27.4	13.9	27.0	16.0/37.0	69.2	58.8	59.0	43.0/84.0
Ele_b_max*(μm)	13.6	7.5	12.0	9.0/16.0	18.7	9.9	16.0	11.0/26.0	31.4	12.3	31.0	22.0/38.0	72.0	35.8	63.0	48.0/89.0
rpi_min	0.7	0.2	0.7	0.6/0.8	0.8	1.4	0.8	0.7/1.0	0.7	2.9	1.1	0.7/1.5	2.0	3.4	1.7	1.3/2.4
rpi_max	1.3	0.4	1.2	1.1/1.4	1.7	1.1	1.5	1.3/1.9	2.5	2.3	2.1	1.8/2.6	4.2	4.6	3.1	2.3/4.2
rpi_avg	1.0	0.3	1.0	0.9/1.1	1.2	0.4	1.1	1.0/1.3	1.5	0.6	1.4	1.1/1.8	2.7	2.1	2.2	1.7/2.8
ART_min	787.5	200.5	776.5	677/899	670.7	272.9	627.0	492/794	494.9	243.2	483.0	317/650	296.4	176.2	270.0	183/387
ART_max	437.6	100.1	443.5	395/502	349.1	115.0	338.5	268/434	251.1	121.9	244.0	182/275	158.1	84.8	148.0	107/209
ART_avg	548.2	116.8	553.0	490/626	463.5	139.6	456.5	370/552	347.1	145.9	340.0	262/416	221.7	114.3	204.0	151/286
Pachy_min (μm)	534.6	35.8	534.0	514/557	510.5	38.3	514.5	484/535	493.3	44.8	494.0	465/524	451.4	62.2	459.0	426/490
Pachy_Apex (μm)	539.5	35.4	539.0	519/561	517.8	38.2	519.5	493/544	502.9	43.5	502.0	477/533	472.4	55.9	476.0	449/507
CV_3 mm (mm^3)	3.9	0.3	3.9	3.7/4.0	3.8	0.3	3.8	3.6/3.9	3.7	0.3	3.6	3.5/3.9	3.5	0.3	3.5	3.4/3.7
CV_5 mm (mm^3)	11.4	0.7	11.4	11/11.9	11.0	0.7	11.1	10.5/11.5	10.9	0.8	10.9	10.3/11.5	10.6	0.9	10.6	10.1/11.2
CV_7 mm (mm^3)	24.6	1.5	24.4	23.7/25.5	23.7	1.4	23.8	22–7/24.6	23.6	1.5	23.6	22.6/24.8	23.3	1.7	23.2	22.3/24.3
CV_10 mm (mm^3)	60.2	3.6	60.0	57.6/62.6	58.0	3.5	58.0	55.4/60.0	57.5	3.6	57.3	54.9/59.8	58.0	4.1	57.6	55.0/60.6

K1: flat meridian, K2: steep meridian, Astig: corneal astigmatism, for explanations of all other parameters: see Table 1.
* Calculated for 8 mm diameter.

Table 3. Results of the ROC analyses of the parameters for their discriminative ability between the normal and keratoconus groups.

	Normal versus subclinical eyes					Subclinical versus keratoconus-suspect eyes					Keratoconus-suspect versus manifest keratoconus eyes				
Parameter (unit)	Cut-off	Roc value	Sensitivity	Specificity	P_{adj}†	Cut-off	Roc value	Sensitivity	Specificity	P_{adj}†	Cut-off	Roc value	Sensitivity	Specificity	P_{adj}†
Age	32.0	0.519	0.507	0.485	1.000	34.0	0.536	0.543	0.548	1.000	34.0	0.466	0.454	0.457	1.000
K1 (D)	43.1	0.464	0.445	0.464	0.784	43.2	0.574	0.600	0.589	0.458	44.1	0.711	0.628	0.629	0.000
K2 (D)	44.5	0.471	0.452	0.459	1.000	45.0	0.671	0.600	0.623	0.002	46.7	0.758	0.717	0.714	0.000
Astig (D)	1.1	0.483	0.445	0.459	1.000	1.3	0.696	0.600	0.596	0.000	2.7	0.669	0.638	0.629	0.007
Kmax (D)	45.4	0.547	0.527	0.551	0.449	46.7	0.762	0.686	0.685	0.000	51.4	0.843	0.771	0.771	0.000
BAD_D	1.4	0.712	**0.658**	**0.658**	0.000	3.2	0.786	**0.743**	**0.740**	0.000	6.0	0.864	**0.799**	***0.800***	0.000
BFS front* (mm)	7.8	0.538	0.527	0.546	0.706	7.8	0.398	0.457	0.404	0.115	7.6	0.243	0.321	0.314	0.000
BFS back* (mm)	6.4	0.566	0.555	0.551	0.117	6.4	0.407	0.429	0.425	0.229	6.3	0.259	0.338	0.343	0.000
Ele_f_Apex*(μm)	3.0	0.515	0.432	0.602	1.000	3.0	0.586	0.514	0.568	0.483	6.0	0.715	0.662	0.657	0.000
Ele_f_TP*(μm)	4.0	0.675	0.548	0.684	0.000	7.0	0.747	0.686	0.740	0.000	15.0	0.902	**0.850**	***0.800***	0.000
Ele_f_max*(μm)	6.0	0.636	0.637	0.566	0.000	10.0	0.828	**0.771**	**0.719**	0.000	20.0	0.928	**0.863**	***0.857***	0.000
Ele_b_Apex*(μm)	3.0	0.545	0.562	0.510	0.503	5.0	0.650	0.629	0.637	0.045	17.0	0.688	0.611	0.629	0.000
Ele_b_TP*(μm)	7.0	0.697	0.637	0.628	0.000	18.0	0.781	0.714	0.692	0.000	40.0	0.881	**0.799**	***0.800***	0.000
Ele_b_max*(μm)	14.0	0.663	0.610	0.622	0.000	25.0	0.796	0.686	0.705	0.000	42.0	0.909	**0.846**	***0.857***	0.000
rpi_min	0.7	0.657	0.637	0.653	0.000	0.9	0.679	0.657	0.651	0.006	1.4	0.784	0.683	0.686	0.000
rpi_max	1.3	0.712	**0.664**	**0.668**	0.000	1.9	0.770	**0.743**	**0.740**	0.000	2.5	0.771	0.686	0.686	0.000
rpi_avg	1.0	0.669	0.623	0.643	0.000	1.2	0.727	0.657	0.658	0.000	1.7	0.795	0.720	0.714	0.000
ART_min	725.0	0.317	0.370	0.367	0.000	551.0	0.303	0.314	0.315	0.001	341.0	0.236	0.328	0.314	0.000
ART_max	412.0	0.272	**0.308**	**0.306**	0.000	275.0	0.235	**0.257**	**0.267**	0.000	192.0	0.227	0.314	0.314	0.000
ART_avg	522.0	0.305	0.342	0.342	0.000	391.0	0.261	0.314	0.315	0.000	274.0	0.228	0.294	0.286	0.000
Pachy_min (μm)	524.0	0.323	0.363	0.357	0.000	503.0	0.375	0.371	0.370	0.074	478.0	0.284	0.328	0.314	0.000
Pachy_Apex (μm)	530.0	0.340	0.384	0.378	0.000	513.0	0.393	0.400	0.390	0.160	490.0	0.326	0.369	0.371	0.000
CV_3 mm (mm^3)	3.9	0.352	**0.349**	**0.423**	0.000	3.8	0.409	0.371	0.432	0.307	3.6	0.356	0.440	0.314	0.008
CV_5 mm (mm^3)	11.3	0.346	0.384	0.393	0.000	11.1	0.456	0.457	0.486	1.000	10.8	0.396	0.416	0.457	0.118
CV_7 mm (mm^3)	24.2	0.340	0.397	0.403	0.000	23.7	0.481	0.486	0.473	1.000	23.5	0.443	0.440	0.429	0.788
CV_10 mm (mm^3)	58.9	0.333	0.397	0.408	0.000	57.7	0.456	0.457	0.459	1.000	57.6	0.530	0.515	0.514	1.000

K1: flat meridian. K2: steep meridian, Astig: corneal astigmatism, for explanations of all other parameters: see Table 1.
The four highest sensitivity/specificity combinations for every tested constellation are emphasized (underlined/bold).
* Calculated for 8 mm diameter.
† *t*-test was applied in the case of normal distribution, otherwise, a nonparametric Mann–Whitney-test was applied. Significant results are marked in grey.

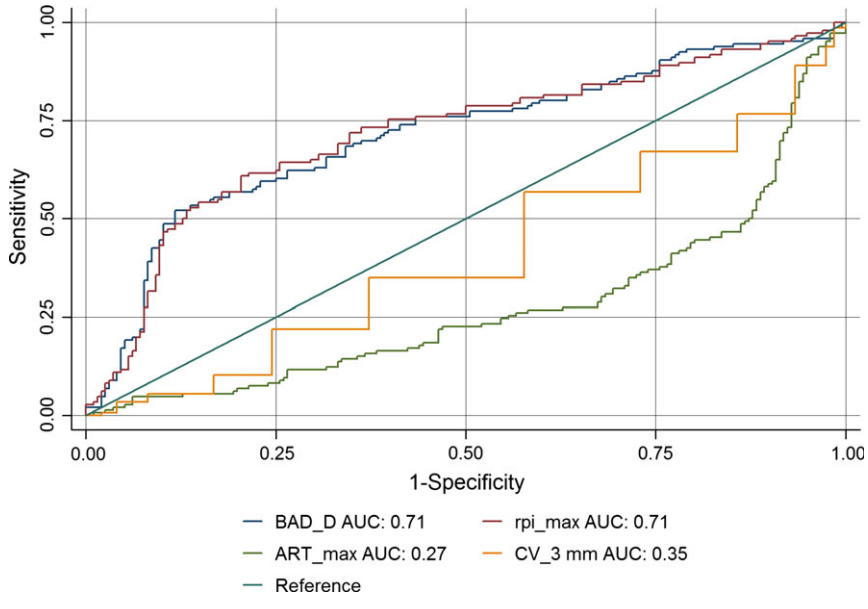

Fig. 1. ROC graphs of the parameters with the highest discriminative ability (normal versus subclinical eyes).

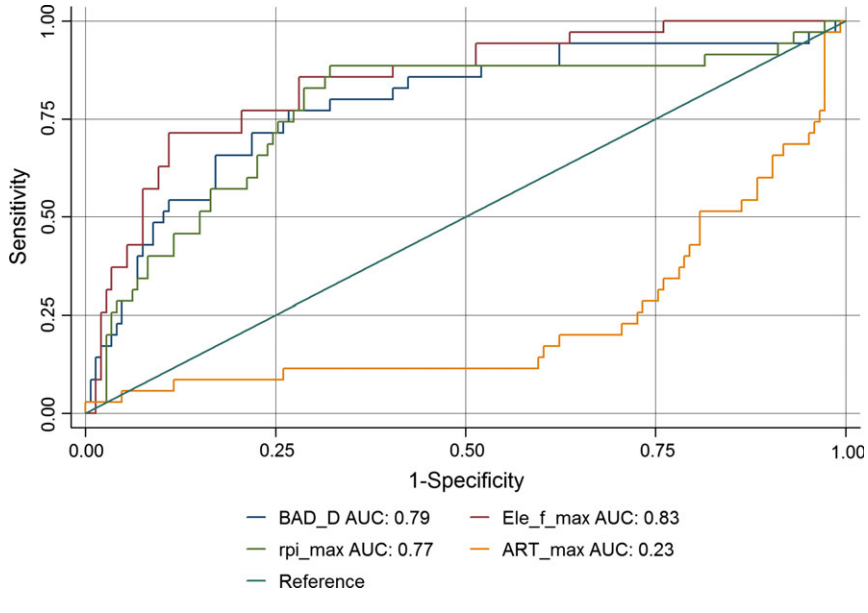

Fig. 2. ROC graphs of the parameters with the highest discriminative ability (subclinical versus keratoconus-suspect eyes).

I, normal eyes (both eyes KISA% <60); group II, subclinical keratoconus (KISA% <60 on subclinical eye with >100 on the fellow eye); group III, keratoconus-suspect (KISA% 60–100); and group IV; clinical manifest keratoconus (KISA% >100).

In addition to the KISA% index, the following data, derived from the Pentacam analysis, were exported to a Microsoft Excel spreadsheet (Table 1):

Informed consent for retrospective data analysis was obtained and the local ethics committee Hamburg, Germany, approved the study. For patients using contact lenses, a minimum of 14 days (hard lenses) or 5 days (soft lenses) of contact lens abstinence was maintained. To avoid a potential bias attributed to diurnal variations of the corneal thickness and the anterior and posterior corneal surface, all the measurements were taken between 12 am and 3 pm (Read et al. 2008). A detailed ophthalmological examination was also performed for each case. Analyses from patients with prior eye surgery, cross-linking therapy, severe sicca syndrome, corneal pathologies other than keratoconus, glaucoma, uveitis or other inflammatory eye diseases were excluded.

Statistical analysis

To avoid a 'between-eye correlation' within the subjects, we randomly selected only one eye for statistical analyses (Armstrong 2013). First, descriptive statistics were analysed for every group. Then, every parameter was tested for normal distribution. If normally distributed, a *t*-test was applied to find potential statistical differences between adjacent groups. If parameters were not normally distributed, a Wilcoxon rank-sum test was applied. Any effect was considered significant if the statistical significance was below 0.05. For differences that were statistically significant, we applied receiver operating characteristics (ROC) to analyse the sensitivity and specificity.

To analyse the correlation and the functional form of the dependence between the tomographic parameters and the KISA% index, we performed robust regression analyses. Additionally, to account for nonlinear dependence, we entered parameters raised to the power of two and three to the right side of the regression equation.

Results

Single eyes from 670 patients (232 women, 438 men) were included into the statistical analyses. The descriptive values are displayed in Table 2. The summary and details of the parameters regarding their discriminative ability between the normal and keratoconus groups (ROC analyses) are displayed in Table 3.

Applying the definition of the groups, none of the topographic parameters demonstrated statistically significant differences between normal and 'subclinical' eyes. However, almost all tomographic parameters displayed statistical significant differences. Comparing 'subclinical', 'keratoconus-suspect' and 'manifest keratoconus' eyes, statistical significant changes could be demonstrated for topographic, as well as for tomographic parameters with increasing sensitivity and specificity. The four highest sensitivity/specificity combina-

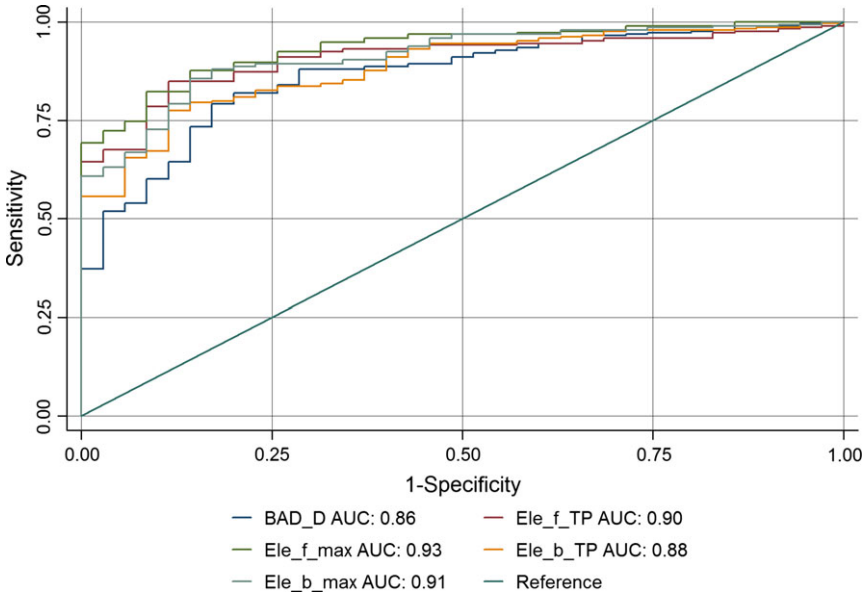

Fig. 3. ROC graphs of the parameters with the highest discriminative ability (keratoconus-suspect versus manifest keratoconus eyes).

tions for every tested constellation are underlined and bold. For the parameters with the highest discriminative ability, the corresponding ROC graphs are displayed in Figs 1–3. It should be borne in mind that the sensitivity/specificity increases with increasing difference to 0.5 (e.g. both a sensitivity of 0.3 and 0.7 have the same discriminative power). If the sensitivity/specificity value is above 0.5, there is a positive correlation between the increase in the groups and the parameter; if the value is below 0.5, there is a negative correlation. This can also be seen from the ROC graphs in Figs 1–3.

To analyse the correlation between the KISA% index and the tomographic parameters, we performed robust regression analyses for the parameters, which showed statistically significant differences in each comparison between adjacent groups. The results for each parameter are displayed in Fig. 4.

All the analysed parameters correlated noticeably with the increasing KISA%. The progression could be precisely demonstrated by a graphical curve based on a mathematical formula displayed in each diagram.

Discussion

This study was initiated to correlate tomographic data to the established KISA% index of Rabinowitz and Rasheed. We demonstrated well-defined correlations between single tomographic parameters (Ele_f_max [$R^2 = 0.70$], Ele_f_TP [$R^2 = .69$], Ele_b_TP [$R^2 = 0.69$]), BAD_D [$R^2 = 0.68$]) and the KISA% index.

The topographic parameters K1, K2, Astig and Kmax did not demonstrate any significant differences between normal and subclinical eyes (see Tables 1 and 2). However, several tomographic parameters demonstrated significant differences between both groups. We identified BAD_D, ART_max, rpi_max and the corneal volume within the central 3 mm (CV_3 mm) as the parameters with the highest discriminative power between normal eyes and subclinical keratoconus. The high discriminative power of the indices BAD_D and ART_max has already been studied, but a major drawback of the recent studies is the inhomogeneous definition and inclusion of keratoconus eyes (Ambrosio et al. 2006, 2011; Ambrosio 2010). Examples are inconclusive statements on definitions, such as comparing 'normal' and 'mild to moderate' keratoconus based on 'classical topographic findings (Ambrosio et al. 2006) or by reporting that the 'diagnosis of keratoconus was made based on Placido-disk-based axial topography, elevation-derived anterior corneal curvature maps and criteria used in the Collaborative Longitudinal Evaluation of Keratoconus (CLEK) study' (Ambrosio et al. 2011). Other studies refer to device-specific grading systems that are not transferable to other devices (Ruisenor Vazquez et al. 2014).

With increasing keratoconus stages, the discriminative power of both BAD_D and ART_max increases (area under the curve [AUC]-$_{\text{BAD\_D normal versus subclinical}} = 0.71$; $\text{AUC}_{\text{BAD\_D subclinical versus suspect}} = 0.79$; $\text{AUC}_{\text{BAD\_D suspect versus manifest}} = 0.86$; $\text{AUC}_{\text{ART\_max normal versus subclinical}} = 0.27$; $\text{AUC}_{\text{ART\_max subclinical versus suspect}} = 0.24$; $\text{AUC}_{\text{ART\_max suspect versus manifest}} = 0.23$). Concomitantly, other tomographic parameters such as ELe_b_max and Ele_f_max and Ele_b_TP increase their sensitivity/specificity and reach their highest discriminative power comparing 'keratoconus-suspect' and 'manifest keratoconus' eyes. The discriminative power of tomographic parameters to differentiate between normal and subclinical keratoconus is moderate albeit statistically significant. The comparison of 'subclinical' and 'keratoconus-suspect' eyes (group II versus group III) demonstrates statistically significant differences between the topographic parameters Astig. and Kmax. This was expected considering that this limit equals the topographically related limit between 'normal' and 'keratoconus-suspect' eyes in the original KISA %-related classification by Rabinowitz and Rasheed (Rabinowitz & Rasheed 1999). Comparing 'subclinical' and 'keratoconus-suspect' eyes, the AUC of single tomographic parameters increases up to values of 0.83 (Ele_f_max). Referring to the original classification of Rabinowitz and Rasheed and comparing 'keratoconus-suspect' eyes with 'normal' eyes, the AUC and the respective sensitivity/specificity would increase further (AUC/sensitivity/specificity for normal versus keratoconus-suspect: BAD_D [0.89/0.89/0.88], ART_max [0.13/0.11/0.11], Ele_f_max [0.89/0.86/0.80]).

Besides defining keratoconus groups based on the KISA% index, Rabinowitz and Rasheed stated that the KISA % is not only a theoretical index, it also has the advantage of a high clinically correlation with the patients visual acuity (Rabinowitz & Rasheed 1999). That the KISA% index also correlates well with the tomographic changes was

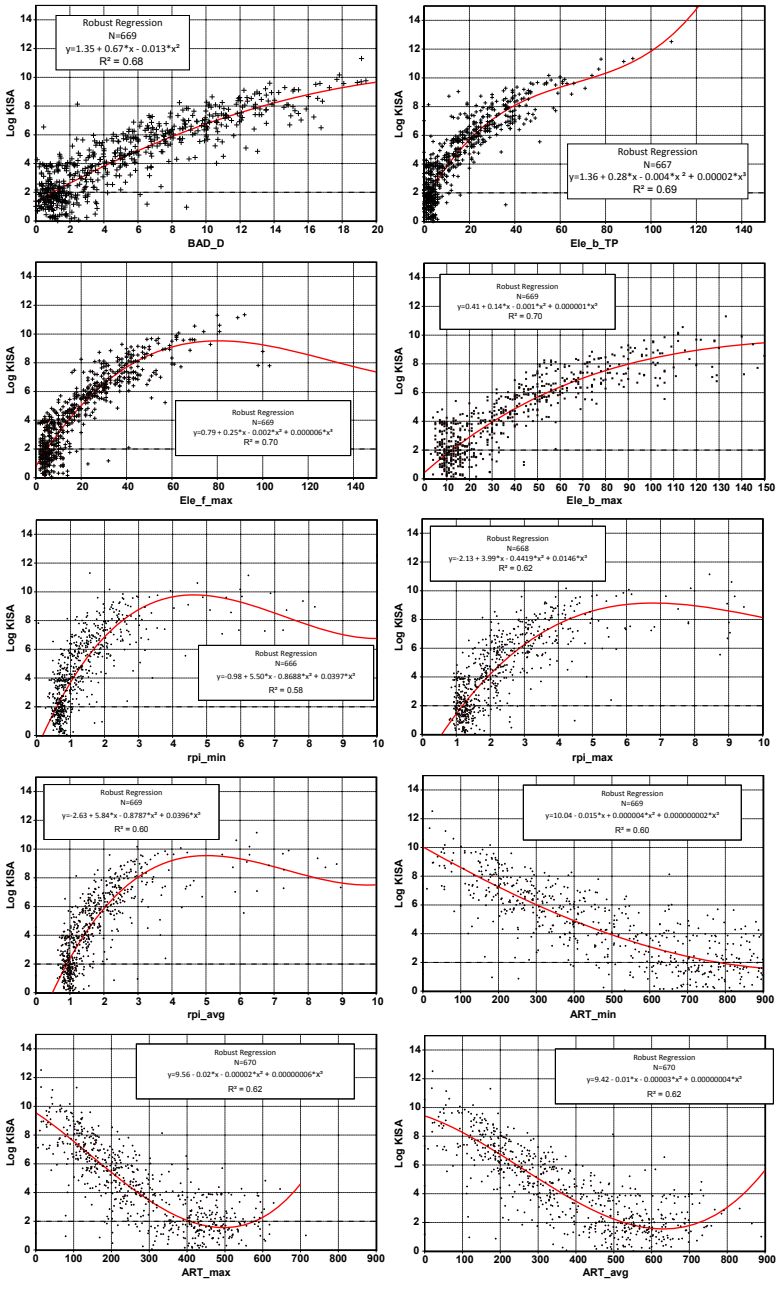

Fig. 4. Results from the robust regression analyses for the tomographic parameters and their correlation with the KISA%.

demonstrated by our robust regression analyses. The highest coefficient of determination (R^2) with the KISA% index, that is the parameters that best explain the increase of the KISA% index in keratoconus eyes, were Ele_f_max ($R^2 = 0.70$), Ele_f_TP ($R^2 = 0.69$), Ele_b_TP ($R^2 = 0.69$) and the BAD_D ($R^2 = 0.68$). Rabinowitz and Rasheed further recommended that 'the KISA% index must be verified by independent observers using different sets of normal control eyes and keratoconus patients. However, if verified, its simplicity will allow it to be used on a universal basis for topographically diagnosing keratoconus using different videokeratoscopes' (Rabinowitz & Rasheed 1999).

Perez et al. stated that 'in corneal refractive surgery, early diagnosis of keratoconus (subclinical asymptomatic keratoconus) is of great importance in patients seeking surgery because it can prevent progression of the pathology after surgery and make it symptomatic (corneal ectasia), thus creating the need for diagnostic tests that provide high sensitivity (ability to detect the disease in affected subjects) with the objective that no asymptomatic subclinical keratoconus ends up not being diagnosed and thus not undergo corneal refractive surgery' (Fernandez Perez et al. 2014). Over the last few years, numerous studies have demonstrated altered tomographic and thickness progression parameters in keratoconus (Tomidokoro et al. 2000; Ambrosio et al. 2006; Fam & Lim 2006; Pinero et al. 2010, 2012; Jhanji et al. 2013). These studies focus mainly on early corneal changes in keratoconus to identify reliable screening parameters. However, the definition and classification of keratoconus is not consistent, which can be misleading because it's not clear, whether the better screening device/parameter/index or the different methodology/classification causes the results.

The KISA% index introduced in 1999 provides an established and 'easy-to-follow' screening method, which is based on parameters of the anterior corneal surface (i.e. topography). In the light of the expanded modern tomographic armamentarium, a new eKISA% classification would now be beneficial. Tomography analyses alone will not help us to identify early keratoconus eyes as soon and as accurately as we need to make the right clinical decisions (Muftuoglu et al. 2013; Mussig et al. 2014; Ruisenor Vazquez et al. 2014). Therefore, current studies combine multiple modalities like corneal tomography, and wavefront and biomechanical analyses to improve the sensitivity and specificity of early keratoconus screening (de Sanctis et al. 2008; Buhren et al. 2010; Arbelaez et al. 2012; Smadja et al. 2013; Ruisenor Vazquez et al. 2014).

The 'gold standard' in keratoconus classification during the last few decades was the 'Amsler-Krumeich Classification' (AKC) (Amsler 1965). This is based on broadly defined topographical and morphological changes diagnosed by keratoscopy and slit-lamp examinations. With the advances in corneal diagnostics and the increasing demand for early keratoconus screening in refractive surgery, the AKC should now only be used in an historical context. Saad et al. recently argued that using different, partially wide-ranging and/or qualitative definitions, insufficient information is gathered to allow other authors to perform similar studies for comparison. They

recommended that to gain a better definition of the keratoconus-suspect topographically, multiple quantitative parameters should be used (Saad & Gatinel 2013). Rabinowitz and Rasheed proposed a KISA% value between 60 and 100% for the diagnosis of keratoconus-suspect. Supporting Saad et al., Sedghipour et al. demonstrated that the KISA% index has a significantly higher sensitivity and specificity than other topographical indices (Sedghipour et al. 2012). Therefore, we followed Saad's recommendation and used the KISA% index to define our groups of 'normal', 'keratoconus-suspect' and 'manifest keratoconus' eyes (Rabinowitz 1995; Rabinowitz & Rasheed 1999).

Today, we have diagnostic devices applying wavefront, tomographic or biomechanical analyses that have the potential to identify corneal changes before topographic changes even occur. Because the KISA% index is based solely on topographic changes, we decided to study the structural changes beneath the surface (i.e. tomographic changes) in eyes with increasing KISA % index.

Recently, Saad and Gatinel pointed out that, as both eyes have the same genetic makeup, in patients with unilateral keratoconus the less-affected eye, although appearing normal, has keratoconus. If observed over a longer period, signs of keratoconus will develop in this eye (Saad & Gatinel 2013). It is important to detect changes indicating keratoconus as early as possible. We, therefore, defined an additional 'subclinical keratoconus' group, defining it as having a KISA% of <60 (subclinical eye) and >100 in the fellow keratoconus eye. Both the normal and the subclinical keratoconus eyes display topography variations within the same 'normal' range, but the subclinical keratoconus eye has an affected fellow eye. We have thus created a new border between 'normal' and 'keratoconus' with respect to the already well-established keratoconus definition based on the KISA% index (Rabinowitz 1995; Rabinowitz & Rasheed 1999). Saad recommended naming keratoconus eyes with no topographical pathologies forme fruste keratoconus (Saad & Gatinel 2010, 2013). However, we prefer the term 'subclinical keratoconus' because these eyes are keratoconus eyes that do not display visual/topographical/clinically relevant changes for the patient, and this definition is easy understandable. The term 'forme fruste' on the other hand was derived historically and, over time, has been used with changing definitions, which complicates a clear understanding (Amsler 1961; Lafond et al. 2001; Alpins & Stamatelatos 2007; Banitt et al. 2011).

After analysing tomographic changes of keratoconus eyes in relation to the KISA% index, we conclude that the well-established KISA% index introduced by Rabinowitz and Rasheed is an excellent index to differentiate between keratoconus stages. This is the first study to systematically analyse tomographic changes in KISA% normal eyes (subclinical keratoconus eyes) and demonstrates the necessity to expand the original KISA% classification. Therefore, we recommend the use of the eKISA% classification' as the foundation for the definition of keratoconus and normal eyes in future keratoconus research projects.

References

Ali NQ, Patel DV & McGhee CN (2014): Biomechanical responses of healthy and keratoconic corneas measured using a noncontact scheimpflug-based tonometer. Invest Ophthalmol Vis Sci **55**: 3651–3659.

Alpins N & Stamatelatos G (2007): Customized photoastigmatic refractive keratectomy using combined topographic and refractive data for myopia and astigmatism in eyes with forme fruste and mild keratoconus. J Cataract Refract Surg **33**: 591–602.

Ambrosio RJ (2010): Simplifying ectasia screening with pentacam corneal tomography. Highlights Ophthalmol **38**: 12–20.

Ambrosio R, Jr, Alonso RS, Luz A & Coca Velarde LG (2006): Corneal-thickness spatial profile and corneal-volume distribution: tomographic indices to detect keratoconus. J Cataract Refract Surg **32**: 1851–1859.

Ambrosio R, Jr, Caiado AL, Guerra FP, Louzada R, Roy AS, Luz A, Dupps WJ & Belin MW (2011): Novel pachymetric parameters based on corneal tomography for diagnosing keratoconus. J Refract Surg **27**: 753–758.

Amsler M (1961): [The "forme fruste" of keratoconus]. Wien Klin Wochenschr **73**: 842–843.

Amsler M (1965): [Early diagnosis and microsymptoms]. Ophthalmologica. Journal international d'ophtalmologie. International journal of ophthalmology. Zeitschrift fur Augenheilkunde **149**: 438–446.

Arbelaez MC, Versaci F, Vestri G, Barboni P & Savini G (2012): Use of a support vector machine for keratoconus and subclinical keratoconus detection by topographic and tomographic data. Ophthalmology **119**: 2231–2238.

Armstrong RA (2013): Statistical guidelines for the analysis of data obtained from one or both eyes. Ophthalmic Physiol Opt **33**: 7–14.

Banitt MR, Romano A, Iragavarapu S, Budenz DL & Lee RK (2011): Forme fruste anterior segment dysgenesis. Br J Ophthalmol, **95**: 1756–1757, 1763.

Buhren J, Kook D, Yoon G & Kohnen T (2010): Detection of subclinical keratoconus by using corneal anterior and posterior surface aberrations and thickness spatial profiles. Invest Ophthalmol Vis Sci **51**: 3424–3432.

Buhren J, Schaffeler T & Kohnen T (2014): Validation of metrics for the detection of subclinical keratoconus in a new patient collective. J Cataract Refract Surg **40**: 259–268.

Fam HB & Lim KL (2006): Corneal elevation indices in normal and keratoconic eyes. J Cataract Refract Surg **32**: 1281–1287.

Fernandez Perez J, Valero Marcos A & Martinez Pena FJ (2014): Early diagnosis of keratoconus: what difference is it making? Br J Ophthalmol **98**: 1465–1466.

Jhanji V, Yang B, Yu M, Ye C & Leung CK (2013): Corneal thickness and elevation measurements using swept source optical coherence tomography and slit scanning topography in normal and keratoconic eyes. Clin Experiment Ophthalmol **41**: 735–745.

Lafond G, Bazin R & Lajoie C (2001): Bilateral severe keratoconus after laser in situ keratomileusis in a patient with forme fruste keratoconus. J Cataract Refract Surg **27**: 1115–1118.

Muftuoglu O, Ayar O, Ozulken K, Ozyol E & Akinci A (2013): Posterior corneal elevation and back difference corneal elevation in diagnosing forme fruste keratoconus in the fellow eyes of unilateral keratoconus patients. J Cataract Refract Surg **39**: 1348–1357.

Mussig L, Zemova E, Pattmoller J, Seitz B, Eppig T, Szentmary N & Langenbucher A (2014): [A Comparison of Device-Based Diagnostic Methods for Keratoconus.]. Klin Monbl Augenheilkd [Epub ahead of print].

Pinero DP, Alio JL, Aleson A, Escaf Vergara M & Miranda M (2010): Corneal volume, pachymetry, and correlation of anterior and posterior corneal shape in subclinical and different stages of clinical keratoconus. J Cataract Refract Surg **36**: 814–825.

Pinero DP, Nieto JC & Lopez-Miguel A (2012): Characterization of corneal structure in keratoconus. J Cataract Refract Surg **38**: 2167–2183.

Rabinowitz YS (1995): Videokeratographic indices to aid in screening for keratoconus. J Refract Surg **11**: 371–379.

Rabinowitz YS (1998): Keratoconus. Surv Ophthalmol **42**: 297–319.

Rabinowitz YS & Rasheed K (1999): KISA% index: a quantitative videokeratography algorithm embodying minimal topographic criteria for diagnosing keratoconus. J Cataract Refract Surg **25**: 1327–1335.

Read SA, Collins MJ & Iskander DR (2008): Diurnal variation of axial length, intraocular pressure, and anterior eye biometrics. Invest Ophthalmol Vis Sci **49**: 2911–2918.

Ruisenor Vazquez PR, Galletti JD, Minguez N, Delrivo M, Fuentes Bonthoux F, Pfortner T & Galletti JG (2014): Pentacam scheimpflug tomography findings in topographically normal patients and subclinical keratoconus cases. Am J Ophthalmol **158**: 32–40 e32.

Saad A & Gatinel D (2010): Topographic and tomographic properties of forme fruste keratoconus corneas. Invest Ophthalmol Vis Sci **51**: 5546–5555.

Saad A & Gatinel D (2013): Subclinical keratoconus: the need for an objective classification system. Ophthalmology **120**: e56–e57.

de Sanctis U, Loiacono C, Richiardi L, Turco D, Mutani B & Grignolo FM (2008): Sensitivity and specificity of posterior corneal elevation measured by Pentacam in discriminating keratoconus/subclinical keratoconus. Ophthalmology **115**: 1534–1539.

Sedghipour MR, Sadigh AL & Motlagh BF (2012): Revisiting corneal topography for the diagnosis of keratoconus: use of Rabinowitz's KISA% index. Clin Ophthalmol **6**: 181–184.

Smadja D, Touboul D, Cohen A, Doveh E, Santhiago MR, Mello GR, Krueger RR & Colin J (2013): Detection of subclinical keratoconus using an automated decision tree classification. Am J Ophthalmol **156**: 237–246 e231.

Tomidokoro A, Oshika T, Amano S, Higaki S, Maeda N & Miyata K (2000): Changes in anterior and posterior corneal curvatures in keratoconus. Ophthalmology **107**: 1328–1332.

Received on January 21st, 2014.
Accepted on October 6th, 2014.

Correspondence:
Johannes Steinberg, MD
Department of Ophthalmology
University Medical Center Hamburg-Eppendorf
Martinistrasse 52, 20246 Hamburg, Germany
Tel: +49 40 4291 6066
Fax: +49 40 7410 54906
Email: johannes.steinberg@gmail.com

Steinberg and Aubke-Schultz contributed equally.